nature neuroscience

Plexin-A2 and its ligand, Sema6A, control nucleus-centrosome coupling in migrating granule cells

Julie Renaud[1,2], Géraldine Kerjan[1,2], Itsuko Sumita[3], Yvrick Zagar[1,2], Virginie Georget[2,4], Doyeun Kim[5], Coralie Fouquet[1,2], Kazunori Suda[3], Makoto Sanbo[6], Fumikazu Suto[7], Susan L Ackerman[5], Kevin J Mitchell[8], Hajime Fujisawa[3] & Alain Chédotal[1,2,9,10]

During their migration, cerebellar granule cells switch from a tangential to a radial mode of migration. We have previously demonstrated that this involves the transmembrane semaphorin Sema6A. We show here that plexin-A2 is the receptor that controls Sema6A function in migrating granule cells. In plexin-A2–deficient (*Plxna2*$^{-/-}$) mice, which were generated by homologous recombination, many granule cells remained in the molecular layer, as we saw in *Sema6a* mutants. A similar phenotype was observed in mutant mice that were generated by mutagenesis with *N*-ethyl-*N*-nitrosourea and had a single amino-acid substitution in the semaphorin domain of plexin-A2. We found that this mutation abolished the ability of Sema6A to bind to plexin-A2. Mouse chimera studies further suggested that plexin-A2 acts in a cell-autonomous manner. We also provide genetic evidence for a ligand-receptor relationship between Sema6A and plexin-A2 in this system. Using time-lapse video microscopy, we found that centrosome-nucleus coupling and coordinated motility were strongly perturbed in *Sema6a*$^{-/-}$ and *Plxna2*$^{-/-}$ granule cells. This suggests that semaphorin-plexin signaling modulates cell migration by controlling centrosome positioning.

In the postnatal mouse cerebellum, granule cells are produced in the external granule cell layer (EGL), where they migrate tangentially and extend two axons parallel to the cerebellum surface (the parallel fibers) before descending through the molecular layer along radial glia fibers[1]. As in other developing neurons, the centrosome has been shown to be important at different phases of granule cell differentiation *in vitro*. First, it controls the appearance of granule cell axons[2]. Second, it orchestrates the nucleokinesis of granule cells during their radial migration[3,4]. Consistent with this, the radial migration of granule cells is abnormal when the expression of centrosomal proteins is perturbed[3,5]. Although extracellular proteins, such as axon guidance molecules, orient migrating neurons in the nervous system, it is still unclear how they influence the migration machinery at a subcellular level[6].

We have recently shown that the switch from tangential to radial migration in cerebellar granule cells is controlled by the transmembrane semaphorin Sema6A acting as a ligand expressed on granule cells[7]. The identity of the Sema6A receptor and its mechanism of action were unknown. In vertebrates, the plexin proteins, four classes (A–D) of which have been defined, are both co-receptors for secreted semaphorins and direct receptors for transmembrane semaphorins[8]. Type A plexins (A1–A4) are the signal transducing components of the receptor complex for most class 3 secreted semaphorins, although these do not bind to type A plexins, but rather to their co-receptors, the neuropilins. However, in the developing heart, plexin-A1 directly binds to Sema6D to control cell migration[9]. Likewise, Sema6A binds to plexin-A4 and plexin-A2 in transfected cells[10,11]. Thus, type A plexins may also be obligate receptors for class 6 semaphorins during axon guidance and cell migration[10,11]. Sema6D can also trigger reverse signaling after binding plexin-A1 (ref. 9).

We show here that plexin-A2 is the receptor that mediates Sema6A function in migrating granule cells, providing direct *in vivo* evidence for a role for type A plexins in neuronal migration. We also show that granule cell nucleokinesis is perturbed in *Plxna2* mutants, as it is in *Sema6a* mutants. Our results suggest that semaphorins and plexins control neuronal migration through the regulation of centrosome-nucleus translocation.

RESULTS

Plexin-A2 is expressed in the developing EGL

It was recently shown that Sema6A binds to plexin-A2 and plexin-A4 in transfected cells[10,11]. To determine whether these plexins could be receptors for Sema6A in the developing cerebellar cortex, we first studied their expression by *in situ* hybridization. We found that only *Plxna2* transcripts were expressed in the postnatal cerebellum (**Fig. 1a**

[1]Centre National de la Recherche Scientifique, UMR7102, 9 Quai Saint-Bernard, Paris F-75005, France. [2]Université Pierre et Marie Curie–Paris 6, UMR7102, Paris F-75005, France. [3]Division of Biological Science, Nagoya University Graduate School of Science, Nagoya 468-8602, Japan. [4]Institut Fédératif de Biologie Intégrative, 9 Quai Saint-Bernard, Paris F-75005, France. [5]Howard Hughes Medical Institute, Jackson Laboratory, 600 Main Street, Bar Harbor, Maine 04609, USA. [6]Laboratory of Neurobiology and Behavioral Genetics, National Institute for Physiological Science, Myodaiji, Okazaki 444-8585, Japan. [7]Division of Developmental Genetics, National Institute of Genetics, Mishima 411-8540, Japan. [8]Smurfit Institute of Genetics, Trinity College Dublin, Dublin 2, Ireland. [9]AP-HP, Groupe Hospitalier Pitié-Salpétrière, Fédération de Neurologie, 91 Boulevard de l'Hôpital, Paris F-75013, France. [10]Present address: Institut de la Vision, INSERM, UMR_S592, 17 rue Moreau, Paris F-75012, France. Correspondence should be addressed to A.C. (chedotal@infobiogen.fr).

Received 15 November 2007; accepted 5 February 2008; published online 9 March 2008; doi:10.1038/nn2064

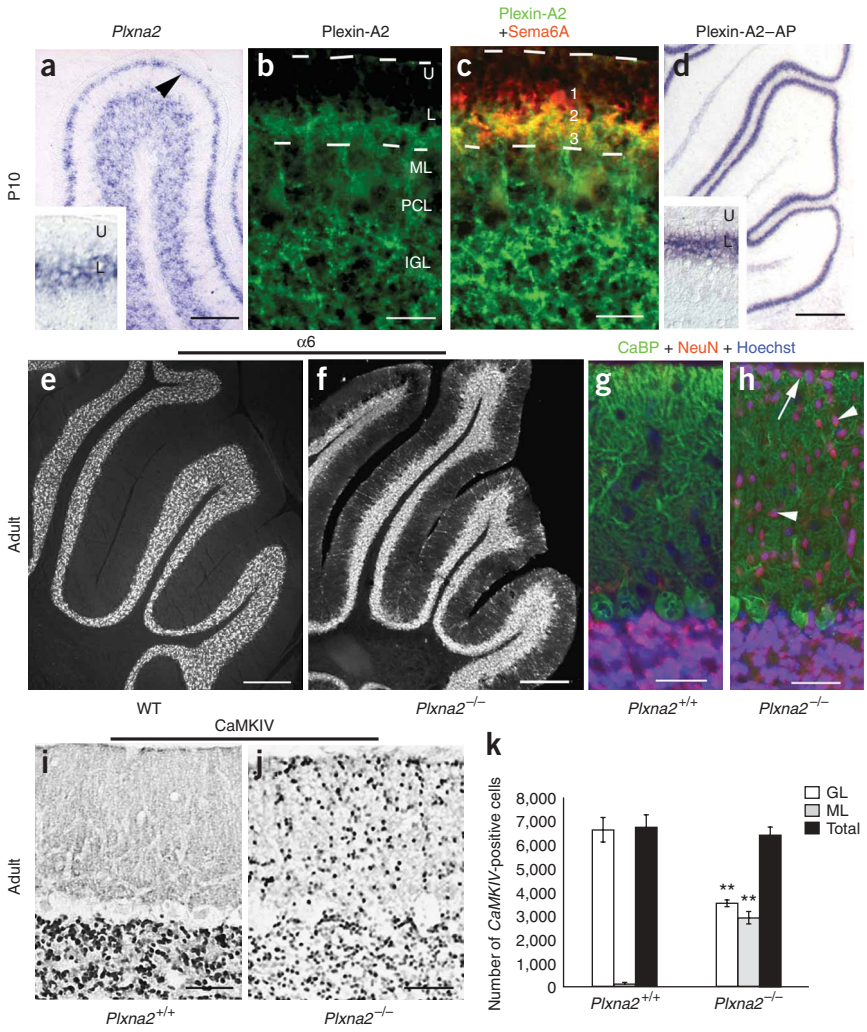

Figure 1 Plexin-A2 expression and function in migrating granule cells. (**a**–**c**) At P10, granule cells in the lower EGL (L; arrowhead in **a**), the molecular layer and the IGL expressed plexin-A2 mRNA (**a**) and protein (**b**,**c**). Double immunostaining for Sema6A and plexin-A2 (**c**) showed that granule cells sequentially expressed Sema6A (1), Sema6A and plexin-A2 (2), and then only plexin-A2 (3). The dashed lines delineate the EGL. (**d**) At P10, plexin-A2–AP bound to the lower EGL. (**e**,**f**) In adult wild-type mice (**e**), all α6-positive granule cells were in the IGL, whereas in *Plxna2*$^{-/-}$ mice (**f**), many α6-positive ectopic granule cells were observed in the molecular layer. (**g**) In wild-type (*Plxna2*$^{+/+}$) mice, NeuN-positive cells were in the IGL, under CaBP-labeled Purkinje cells. (**h**) In *Plxna2*$^{-/-}$ mice, many NeuN-positive cells were in the molecular layer (arrowheads) or at the pial surface (arrow). (**i**,**j**) *Plxna2*$^{+/+}$ (**i**) or *Plxna2*$^{-/-}$ (**j**) cerebella immunostained for CaMKIV. (**k**) Quantification of the number of CaMKIV-positive granule cells in the granule cell layer (GL) and the molecular layer (ML; **, $P < 0.005$ to *Plxna2*$^{+/+}$). PCL, Purkinje cell layer; U, upper EGL. Scale bars represent 100 μm (**a**), 35 μm (**b**,**c**,**g**,**h**), 50 μm (**i**,**j**), 300 μm (**d**) and 500 μm (**e**,**f**). Error bars represent s.e.m.

and data not shown). Immunostaining with antibodies to plexin-A2 (ref. 11) revealed that plexin-A2 was expressed by granule cells in the lower EGL, molecular layer and internal granule cell layer (IGL; **Fig. 1b**). Double staining for Sema6A and plexin-A2 showed that migrating granule cells first expressed only Sema6A in the lower EGL, then both Sema6A and plexin-A2, and finally only plexin-A2 on leaving the EGL (**Fig. 1c**). Moreover, a recombinant protein encoding the plexin-A2 Sema domain fused to alkaline-phosphatase (plexin-A2–AP) bound exclusively to the lower EGL, where Sema6A was expressed (**Fig. 1d**). These data indicate that plexin-A2 and Sema6A could interact in the EGL.

Abnormal granule cell migration in plexin-A2–deficient mice

We next studied cerebellum organization in a *Plxna2* knockout line that was generated by homologous recombination and that is a protein null mutant[11] (*Plxna2*$^{-/-}$). *Plxna2*$^{-/-}$ homozygous mutant mice were viable and fertile. The outward appearance of their cerebellum was indistinguishable from that of wild-type mice (data not shown). However, immunohistochemical analysis of the adult cerebella showed that many granule cells were in the molecular layer in *Plxna2*$^{-/-}$ mice and not in wild-type or *Plxna2*$^{+/-}$ mice (**Fig. 1e–k** and data not shown). The ectopic granule cells expressed the same markers as fully differentiated granule cells, such as α6 $GABA_A$ receptor subunit (α6; **Fig. 1f**), the nuclear protein NeuN[12] (**Fig. 1g**,**f**) and Ca^{2+}/calmodulin-dependent protein kinase IV[13] (CaMKIV; **Fig. 1i**,**j**). Quantification of CaMKIV-positive granule cells indicated that about 40% of the granule cells remained in the molecular layer in *Plxna2*$^{-/-}$ mice (**Fig. 1k**). Bromodeoxyuridine (BrdU) pulse labeling confirmed that there was a substantial reduction in the number of granule cells that had left the EGL at 36 h after the injection, and that about one-third of the postmitotic granule cells were still in the EGL after 100 h, versus 5% in wild type (**Supplementary Fig. 1** online). This also showed that their proliferation and survival were not affected (data not shown). Likewise, the differentiation of Purkinje cells, the postsynaptic partner of granule cells, the number of molecular layer interneurons, and the organization of radial glia fibers were all similar to what was observed in wild-type animals. Finally, ectopic granule cells were still innervated by mossy fibers (**Fig. 1g**,**h** and data not shown).

In EGL microexplant cultures, granule cells migrate out tangentially without glial support[7]. Plexin-A2 and Sema6A appeared to be homogeneously expressed on the surface of migrating granule cells (**Supplementary Fig. 2** online). The number of migrating granule cells was considerably reduced using EGL explants from plexin-A2–deficient mice (**Fig. 2**). The maximum migration distance after 48 h (the external limit of the region that comprised 90% of the granule cells) was also significantly reduced for the *Plxna2*$^{-/-}$ granule cells (158.9 ± 4.6 μm, $n = 43$ explants) compared with the *Plxna2*$^{+/-}$ granule cells (256.7 ± 3.4 μm, $n = 29$ explants, $P < 0.0001$). In contrast, neurite outgrowth from *Plxna2*$^{-/-}$ granule cells was normal (**Fig. 2** and data not shown). In *Plxna2*$^{-/-}$ explants, the total neuritic length (665 ± 2.7 μm, $n = 12$ explants) and the length of the longest neurite (896 ± 14.9 μm, $n = 30$ explants) were not significantly different from *Plxna2*$^{+/-}$ (665.5 ± 2.5 μm, $n = 12$ explants; 887.2 ± 29.6 μm, $n = 34$ explants; $P = 0.37$ and $P = 0.45$, respectively).

We next analyzed a mutant line, *NMF454*, that was identified in a recessive, genome-wide *N*-ethyl-*N*-nitrosourea (ENU) mutagenesis

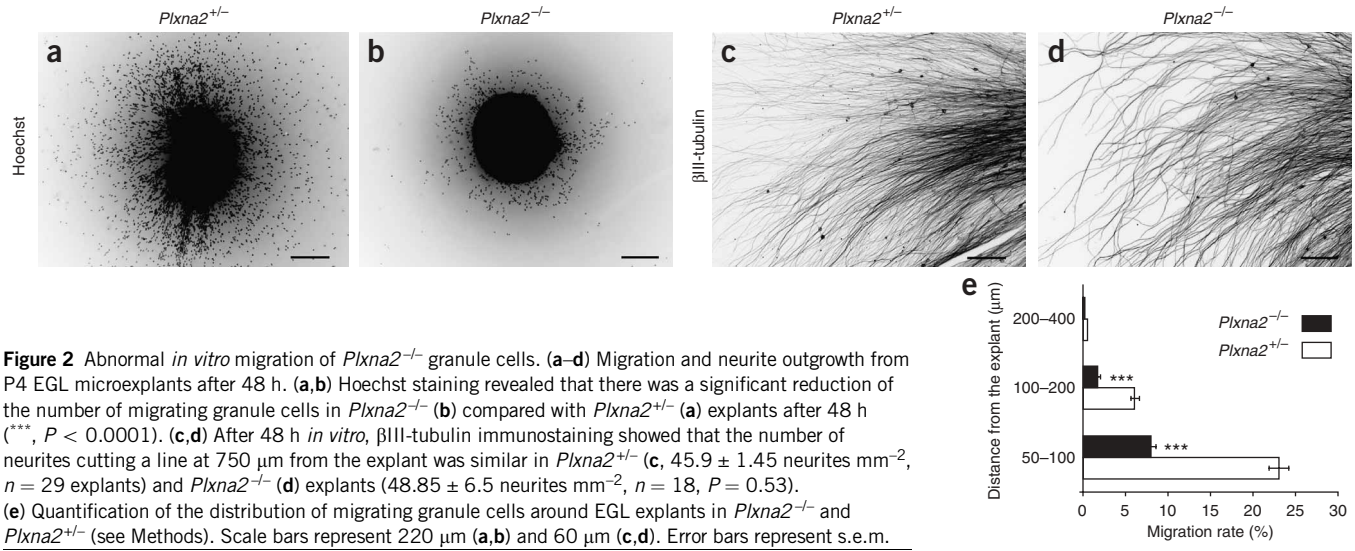

Figure 2 Abnormal *in vitro* migration of *Plxna2*$^{-/-}$ granule cells. (**a**–**d**) Migration and neurite outgrowth from P4 EGL microexplants after 48 h. (**a**,**b**) Hoechst staining revealed that there was a significant reduction of the number of migrating granule cells in *Plxna2*$^{-/-}$ (**b**) compared with *Plxna2*$^{+/-}$ (**a**) explants after 48 h (***, $P < 0.0001$). (**c**,**d**) After 48 h *in vitro*, βIII-tubulin immunostaining showed that the number of neurites cutting a line at 750 μm from the explant was similar in *Plxna2*$^{+/-}$ (**c**, 45.9 ± 1.45 neurites mm^{-2}, $n = 29$ explants) and *Plxna2*$^{-/-}$ (**d**) explants (48.85 ± 6.5 neurites mm^{-2}, $n = 18$, $P = 0.53$). (**e**) Quantification of the distribution of migrating granule cells around EGL explants in *Plxna2*$^{-/-}$ and *Plxna2*$^{+/-}$ (see Methods). Scale bars represent 220 μm (**a**,**b**) and 60 μm (**c**,**d**). Error bars represent s.e.m.

screen of C57BL6/J mice (see Methods). Histological analysis of *NMF454* mutant mice revealed a hypercellular molecular layer of the cerebellum that appeared to be markedly similar to that of the *Plxna2*$^{-/-}$ and *Sema6a*$^{-/-}$ mice. Accordingly, many ectopic NeuN- and α6-positive granule cells were detected in the molecular layer of *NMF454* mutant mice (**Fig. 3a–d**).

To determine whether the *NMF454* mutation resides in either the *Plxna2* or *Sema6a* gene, we first determined whether the phenotype segregated with markers closely linked to these genes. Affected F2 offspring ($n = 11$) from an intercross of F_1 progeny from a mapping cross (C57BL6/J × BALB/cBy) were identified histologically and then genotyped with the polymorphic microsatellite markers *D1Mit155* and *D18Mit178*, which are closely linked to the *Plxna2* and *Sema6a* genes, respectively. No linkage was found with *D18Mit178* ($\chi^2 = 1.2$, $P > 0.5$). However, tight linkage was observed with *D1Mit155* ($\chi^2 = 33.0$, $P < 0.0001$). This result, combined with the phenotypic analysis, suggested that the *NMF454* mutation resides in the *Plxna2* gene.

Western blot analysis of plexin-A2 expression in the cerebellum and neocortex revealed that a ~250-kDa band was present in *NMF454* homozygous mutant, wild-type and *NMF454* heterozygous control ($n = 2$ animals per genotype) mice, but not in *Plxna2*$^{-/-}$ mice[11]

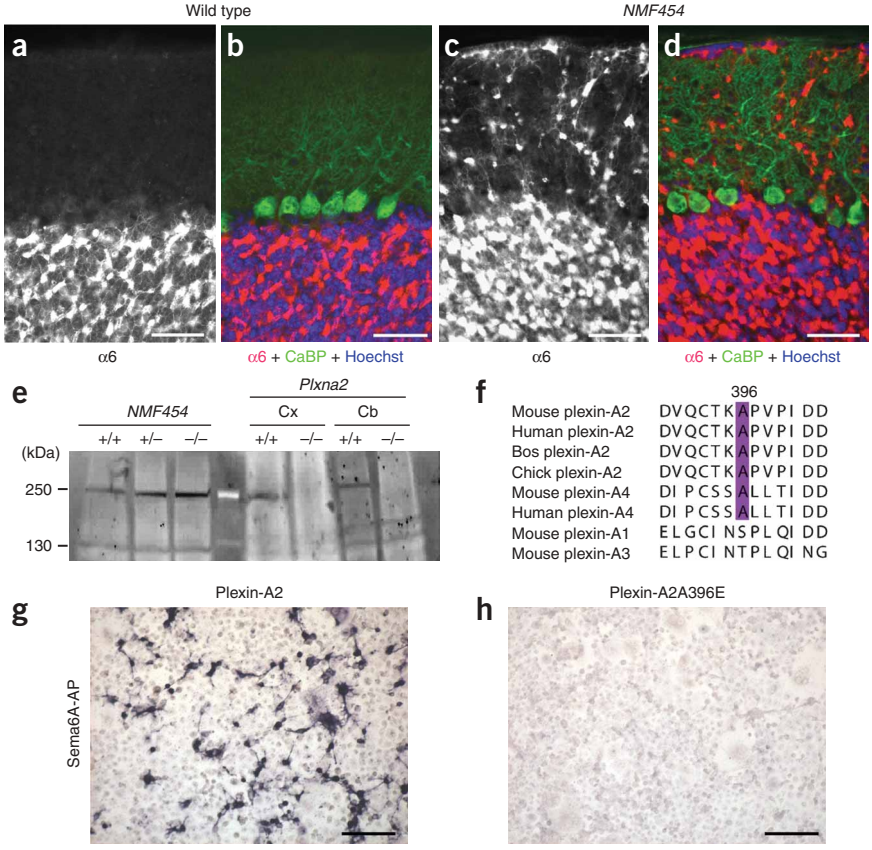

Figure 3 Analysis of *NMF454* ENU-*Plxna2* mutants. (**a**–**d**) Sagittal sections of the cerebella of adult wild-type (WT) and *NMF454* homozygous mice, immunolabeled with antibodies to α6 (**a**–**d**) and CaBP (**b**,**d**) and counterstained with Hoechst (**b**,**d**). Many ectopic α6-positive granule cells were detected in the molecular layer of *NMF454* mutants, whereas they were all in the IGL in wild type. (**e**) Immunoblot analysis of plexin-A2 expression in the two *Plxna2* mutant lines using antibodies to plexin-A2. A band of 250 kDa is detected in cerebellar (Cb) or cortical (Cx) extracts from wild-type (+/+), *NMF454* heterozygous (+/–) and *NMF454* homozygous (–/–) mice. In contrast, the 250-kDa band is absent from cortical and cerebellar extracts from the protein-null *Plxna2* knockout[11]. (**f**) Alignment of type A plexin amino-acid sequences around the *NMF454* mutation site. The alanine in position 396 (purple) is conserved in vertebrate plexin-A2 and plexin-A4 proteins, but is absent from plexin-A1 and A3. In *NMF454* ENU–plexin-A2 mutants, this alanine was replaced by a glutamic acid. (**g**,**h**) Sema6A-AP fusion protein bound to COS cells expressing wild-type plexin-A2, but not to cells expressing A396E mutated plexin-A2 protein. Scale bars represent 35 μm (**a**–**d**) and 600 μm (**g**,**h**).

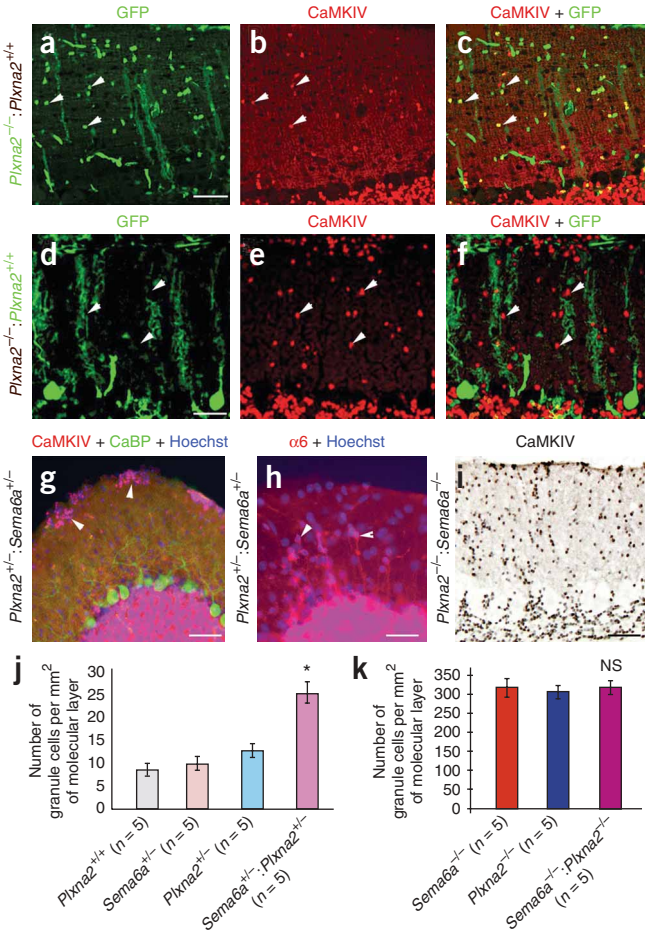

Figure 4 Cell-autonomous function of plexin-A2 in migrating granule cells. (**a**–**f**) Mouse chimera analysis. In *GFP;Plxna2*$^{-/-}$*:Plxna2*$^{+/+}$ chimera, CaMKIV-positive ectopic granule cells were found in the molecular layer and almost all expressed GFP (arrowheads, **a**–**c**). Likewise, in *Plxna2*$^{-/-}$*:Plxna2*$^{+/+}$*;GFP* chimeras, ectopic CaMKIV-positive granule cells in the molecular layer did not express GFP (**d**–**f**). (**g**–**k**) Genetic interaction between *Plxna2* and *Sema6a*. In *Sema6a*$^{+/-}$*;Plxna2*$^{+/-}$ transheterozygotes and *Sema6a*$^{-/-}$*; Plxna2*$^{-/-}$ double homozygotes, ectopic granule cells expressing CaMKIV (**g**–**i**) or α6 (**h**) were found in the molecular layer (arrowheads). (**j**,**k**) Quantification of the number of ectopic granule cells in transheterozygotes and double homozygotes. *, $P < 0.01$; NS, nonsignificant. Scale bars represent 35 μm (**a**–**f**,**i**) and 45 μm (**g**,**h**).

(**Fig. 3e**), suggesting that the ENU mutation did not result in a null allele or a truncated plexin-A2 protein. To further localize the mutation, all exons of the *Plxna2* gene were sequenced from *NMF454* homozygous mutants ($n = 3$) and wild-type controls ($n = 2$). We found a single nucleotide substitution of the cytosine at position 1187 by an adenine, resulting in the replacement of the alanine (396) by a glutamic acid residue (A396E). Notably, this alanine, localized in the semaphorin domain, was evolutionarily conserved in plexin-A2 and plexin-A4 proteins (**Fig. 3f**), to which Sema6A binds[10,11], but was absent from plexin-A1 and plexin-A3 proteins. We used targeted mutagenesis to introduce the same cytosine 1187 point mutation into the plexin-A2 cDNA. This showed that, although Sema6A-AP bound very strongly to COS7 cells expressing wild-type plexin-A2 (**Fig. 3g**), it did not bind at all to cells expressing plexin-A2A396E (**Fig. 3h**).

Cell-autonomous control of neuronal migration by plexin-A2

To determine whether plexin-A2 functions in a cell-autonomous manner, as a receptor in migrating granule cells, we generated *Plxna2*$^{-/-}$*;Plxna2*$^{+/+}$ mouse chimeras. In some chimeras, wild-type cells expressed an actin–green fluorescent protein (GFP) transgene[14]. In other chimeras, cells were used from *Plxna2*$^{-/-}$ mice crossed with actin-GFP transgenics; in these, the mutant cells were identified by their GFP expression. We generated *GFP;Plxna2*$^{-/-}$*:Plxna2*$^{+/+}$ ($n = 5$) and *Plxna2*$^{-/-}$*:GFP;Plxna2*$^{+/+}$ chimeric mice ($n = 3$). The IGL of *GFP;Plxna2*$^{-/-}$*:Plxna2*$^{+/+}$ chimeras contained a mixture of *GFP;Plxna2*$^{-/-}$ and wild-type granule cells (6.2% of CaMKIV-positive granule cells were also GFP positive; **Fig. 4a**–**c**). More than 85% of the ectopic granule cells coexpressed GFP and were thus of *Plxna2*$^{-/-}$ origin (**Fig. 4a**–**c**). Overall 39.4% of the *Plxna2*$^{-/-}$ granule cells (CaMKIV-GFP double labeled) were in the molecular layer and 60.6% were in the IGL, a granule cell distribution comparable to that in *Plxna2*$^{-/-}$ mutant cerebella (see above). Ectopic CaMKIV-expressing granule cells were also detected in the molecular layer of *Plxna2*$^{-/-}$*:Plxna2*$^{+/+}$*;GFP* chimeric mice (**Fig. 4d**–**f**), and 99.5% of the ectopic granule cells did not express GFP and were therefore *Plxna2*$^{-/-}$ (**Fig. 4d**–**f**). In the chimera, only 0.2% of the CaMKIV-GFP double-labeled granule cells (of wild-type origin) were in the molecular layer and 99.8% were in the IGL. This indicates that the block in cell migration that leaves many granule cells stranded in the molecular layer is intrinsic to *Plxna2*$^{-/-}$ neurons. These results strongly suggest that plexin-A2 controls granule cell migration cell-autonomously.

Cyclin-dependent kinase 5 (Cdk5) has previously been shown to associate with the plexin-A2 cytoplasmic domain in the presence of active Src kinase[15]. In addition, Cdk5 phosphorylation is induced downstream of plexin-A2 after Sema3A binding to its co-receptor, neuropilin-1. To further demonstrate that Sema6A can directly signal through plexin-A2 receptor, we applied Sema6A-Fc protein (see Methods) for 10 min to HEK293T cells transfected with plexin-A2, Cdk5 and p35, its coactivator (**Supplementary Fig. 3** online). Immunoblot analysis using antibody to phospho-Cdk5 (Tyr15) showed that Sema6A-Fc induced Cdk5 phosphorylation in a dose-dependent manner in cells expressing plexin-A2/Cdk5/p35 (**Supplementary Fig. 3**). Thus, Sema6A can directly trigger plexin-A2 activation.

We next tried to obtain genetic evidence to support this interaction by generating *Sema6a*$^{+/-}$*;Plxna2*$^{+/-}$ transheterozygous and *Sema6a*$^{-/-}$*; Plxna2*$^{-/-}$ double homozygous mice. In all cases, the numbers of CaMKIV-positive or α6-positive granule cells in the molecular layer of adult mice were quantified (**Fig. 4g**–**k**). Although the number of ectopic granule cells in either *Sema6a*$^{+/-}$ or *Plxna2*$^{+/-}$ single heterozygous mice was similar to that in wild-type mice, there was a significantly increased number of ectopic granule cells in *Sema6a*$^{+/-}$*; Plxna2*$^{+/-}$ double heterozygous mice compared with wild-type ($P < 0.001$), *Sema6a*$^{+/-}$ ($P < 0.001$) or *Plxna2*$^{+/-}$ ($P < 0.005$) mice. Moreover, the number of ectopic granule cells was not significantly increased in *Sema6a*$^{-/-}$*;Plxna2*$^{-/-}$ double mutants compared with *Sema6a*$^{-/-}$ or *Plxna2*$^{-/-}$ single mutants ($P = 0.81$ compared with *Sema6a*$^{-/-}$, $P = 0.48$ compared with *Plxna2*$^{-/-}$; **Fig. 4k**). This further suggests that plexin-A2 and Sema6A act in the same signaling pathway.

Centrosome-nucleus uncoupling in *Plxna2*$^{-/-}$ granule cells

In cerebellar granule cells, as in other cell types, microtubules linked to the centrosome pull the nucleus during migration. In migrating neurons, the movement of the centrosome away from the nucleus in the leading process appears to precede nuclear translocation[16–18]. To try to further characterize granule cell migration defects in *Plxna2*- and

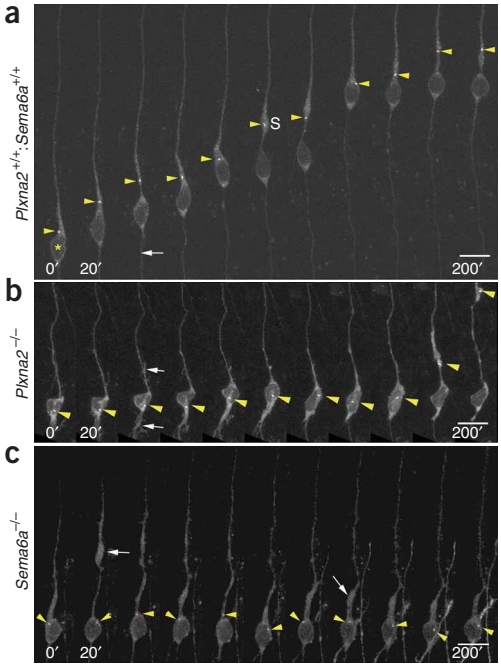

Figure 5 Abnormal nucleus-centrosome coupling in *Sema6a* and *Plxna2* mutants. (**a**–**c**) Time-lapse imaging series (200 min) of migrating granule cells from P5 EGL explants transfected with centrin 1–GFP and cultured for 36 h before imaging. Explants are located on the bottom of the frame (interval between pictures is 20 min). (**a**) In *Plxna2*$^{+/+}$;*Sema6a*$^{+/+}$ mice, the centrosome (arrowhead) appeared as a bright GFP spot just ahead of the nucleus (asterisk). The centrosome transiently moved forward (up), away from the nucleus, inside a swelling (s) of the leading process before the nucleus jumped forward and a new cycle started. The cell has a long trailing process (arrow) that extends caudally from the cell body to the explant surface. (**b**) In *Plxna2*$^{-/-}$ granule cells, the centrosome (arrowhead) turned around the nucleus before rapidly moving away from it, forward, in the leading process. Also note that many side branches (arrows) were present on the surface of the leading and trailing processes. (**c**) In *Sema6a*$^{-/-}$ granule cells, the centrosome (arrowhead) did not separate from the nucleus, although a transient swelling (arrow) can still form in the leading process ahead of the nucleus (see also **Supplementary Videos 1**–**6**). Scale bars represent 8 μm (**a**,**c**) and 10 μm (**b**).

Sema6a-deficient mice, we electroporated constructs encoding the centrosomal protein centrin 1 fused to GFP into P5 cerebella, as has been previously done for other neurons[4,18,19]. EGL explants were dissected immediately after transfection and cultured for 36–48 h. We first measured the distance separating the centrosome from the nucleus (visualized by Hoechst staining). We confirmed the position of the centrosome by immunostaining for γ-tubulin (data not shown). In tangentially migrating granule cells from wild-type and *Plxna2*$^{+/-}$ mice, the centrosome appeared as two neighboring spots that were often localized in a swelling of the leading process ahead of the nucleus (**Figs. 5** and **6**), as has been previously described for other neurons. In 94% of the wild-type cells ($n = 106$), the distance between the centrosome and the nucleus was smaller than 5 μm and never exceeded 10 μm, with a mean distance of 2.29 ± 0.15 μm (**Figs. 5a** and **6a**,**b** and **Supplementary Fig. 4** online). In *Plxna2*$^{-/-}$ granule cells ($n = 112$), the distance between the centrosome and the nucleus was more variable and increased (6 ± 0.66 μm; $P < 0.0001$): only 60% of the cells have a distance smaller than 5 μm, and 21% have a distance larger than 10 μm. A few granule cells had a centrosome at more than 35 μm from the nucleus (**Figs. 5b** and **6a**,**b** and **Supplementary Fig. 4**). In contrast, in *Sema6a*$^{-/-}$ granule cells ($n = 101$), the distance between the centrosome and the nucleus never exceeded 5 μm and was on average significantly shorter (1.23 ± 0.05 μm; $P < 0.0001$; **Figs. 5c** and **6a**,**b** and

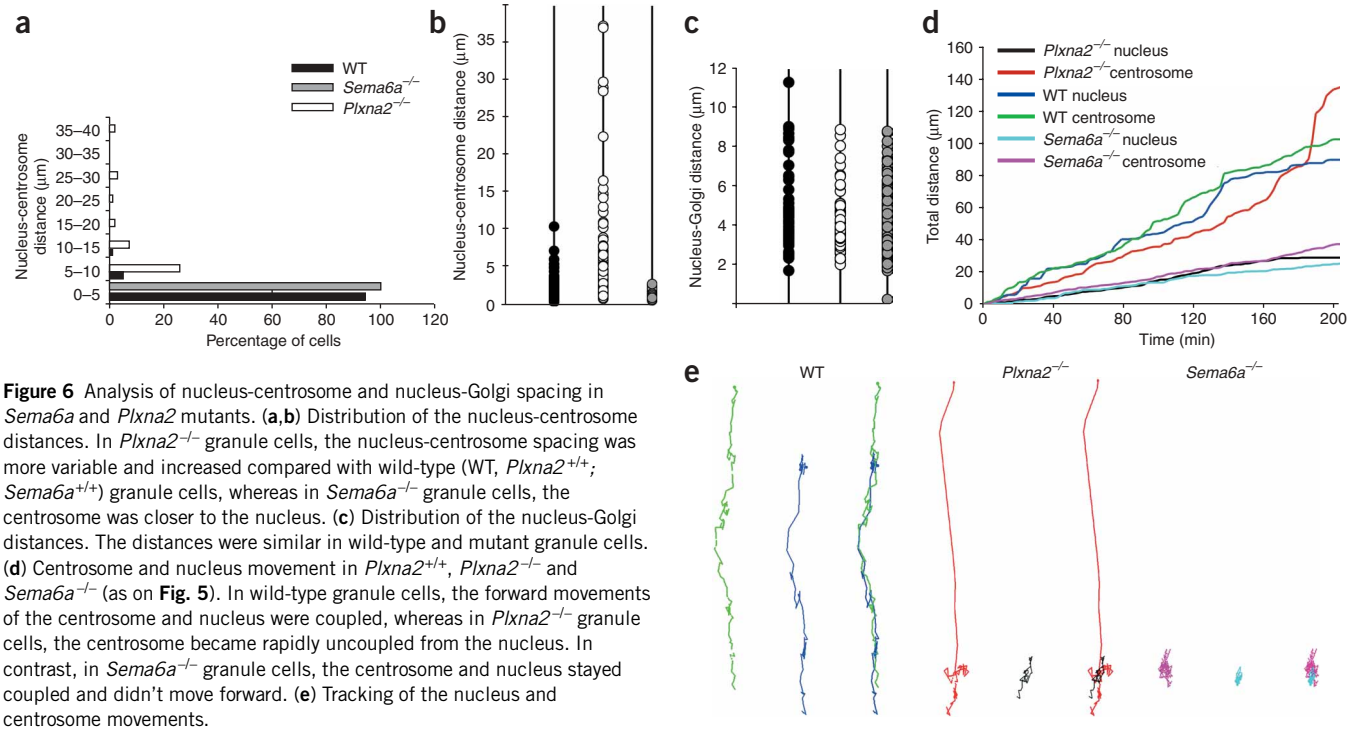

Figure 6 Analysis of nucleus-centrosome and nucleus-Golgi spacing in *Sema6a* and *Plxna2* mutants. (**a**,**b**) Distribution of the nucleus-centrosome distances. In *Plxna2*$^{-/-}$ granule cells, the nucleus-centrosome spacing was more variable and increased compared with wild-type (WT, *Plxna2*$^{+/+}$; *Sema6a*$^{+/+}$) granule cells, whereas in *Sema6a*$^{-/-}$ granule cells, the centrosome was closer to the nucleus. (**c**) Distribution of the nucleus-Golgi distances. The distances were similar in wild-type and mutant granule cells. (**d**) Centrosome and nucleus movement in *Plxna2*$^{+/+}$, *Plxna2*$^{-/-}$ and *Sema6a*$^{-/-}$ (as on **Fig. 5**). In wild-type granule cells, the forward movements of the centrosome and nucleus were coupled, whereas in *Plxna2*$^{-/-}$ granule cells, the centrosome became rapidly uncoupled from the nucleus. In contrast, in *Sema6a*$^{-/-}$ granule cells, the centrosome and nucleus stayed coupled and didn't move forward. (**e**) Tracking of the nucleus and centrosome movements.

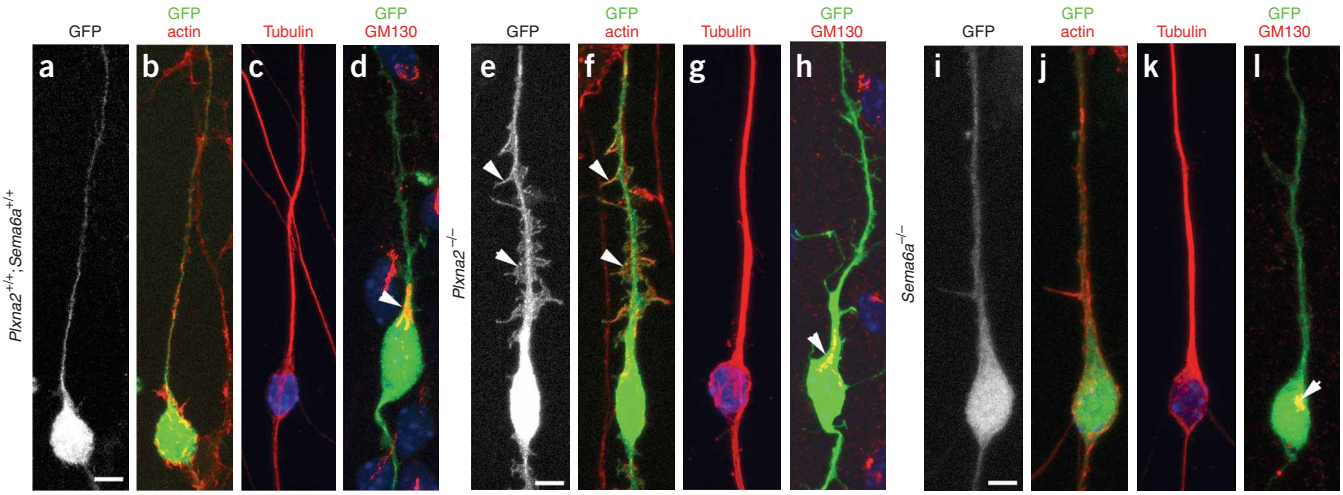

Figure 7 Cytoskeleton and Golgi apparatus in *Sema6a* and *Plxna2* mutant granule cells. (**a**–**l**) GFP-expressing granule cells migrating tangentially were labeled with rhodamine-conjugated phalloidin (**a**,**b**,**e**,**f**,**i**,**j**), or immunolabeled with antibodies to βIII-tubulin (**c**,**g**,**k**) or to GM-130 to stain Golgi apparatus (**d**,**h**,**l**). The explant side is toward the bottom of each panel. (**a**,**b**,**e**,**f**,**i**) In wild-type and Sema6A-deficient granule cells (**a**,**b**,**i**,**j**), the leading and trailing processes were smooth and had only a few actin-rich protrusions. By contrast, the leading and trailing processes of *Plxna2*$^{-/-}$ granule cells were covered with actin-rich protrusions (arrowheads in **e** and **f**). (**c**,**g**,**k**) In all type of granule cells, microtubules were found in the neurites and cell bodies, but in *Plxna2*$^{-/-}$ granule cells, the protrusions were not labeled (**g**). (**d**,**h**,**l**) In all types of granule cells, the Golgi apparatus (arrowhead) stayed at the rostral pole of the nucleus. Scale bars represent 5 μm.

Supplementary Fig. 4). This shows that the distance between the centrosome and the nucleus is abnormal in the absence of plexin-A2 or Sema6A.

In tangentially migrating cortical interneurons and radially migrating granule cells, the forward movements of the centrosome and the Golgi apparatus are coupled[4,16]. To analyze the position of the Golgi apparatus in *Sema6a* and *Plxna2* mutants, we labeled EGL explants with GM-130 antibodies. The distance between the Golgi and the nucleus was not significantly different between wild-type (4.66 ± 0.22 μm, $n = 78$ granule cells) and *Sema6a*$^{-/-}$ (4.26 ± 0.12 μm, $n = 168$ granule cells, $P = 0.95$) or *Plxna2*$^{-/-}$ (4.54 ± 0.19 μm, $n = 90$, $P = 0.1$) granule cells, and was mostly between 2 and 10 μm (**Figs. 6c** and **7**). This suggests that the absence of Sema6A and plexin-A2 selectively perturbs centrosome positioning.

We next carried out time-lapse video microscopy on granule cells expressing centrin 1–GFP after 36–48 h in culture (**Fig. 5a–c**) and performed tracking analysis to evaluate the total distance covered by the centrosome (see Methods). As a result of GFP leakage, the overall morphology of the migrating granule cells could also be visualized, and the nucleus appeared to be a dark, oval-shaped disk filling most of the granule cell soma. In addition, the morphology of individual migrating granule cells was studied using an expression vector encoding enhanced GFP (EGFP, see Methods). Some explants were fixed and stained with rhodamine-conjugated phalloidin or antibody to βIII-tubulin to visualize actin and microtubules, respectively.

In control explants ($n = 16$ explants, eight independent experiments, 2-min interval over 5–6 h), nuclear movement was saltatory and preceded by the appearance of an elongated swelling ahead of the nucleus, as has been described for cortical interneurons[16,18] and radially migrating granule cells[4] (**Supplementary Video 1** online and **Figs. 5a** and **6d**,**e**). This swelling was smooth and localized ahead of the nucleus. Unlike cortical interneurons[16], tangentially migrating granule cells have a long trailing process that always remains attached to the explant (**Figs. 2**, **5a** and **7**). The trailing and leading processes were smooth, bearing only a few actin-rich protrusions (**Fig. 7**), and the forward translocation of the nucleus was always preceded by a forward movement of the centrosome inside the rostral swelling (**Supplementary Videos 1** and **2** online and **Figs. 5a** and **6d**,**e**). The migratory behavior of *Plxna2*$^{-/-}$ granule cells ($n = 11$ explants, three independent experiments, 2-min interval over 3–4 h) was different. First, the rostral swelling and processes bore many dynamic extensions resembling growth cone filopodia (**Fig. 5b** and **Supplementary Videos 3** and **4** online) that were enriched in actin, but did not seem to contain microtubules (**Fig. 7**). Second, the centrosome initially moved into the rostral swelling, but then rapidly detached from it. This was followed by a complete blockade of nuclear movement (**Figs. 5b** and **6d**,**e**).

In explants from *Sema6A*$^{-/-}$ mice ($n = 8$ explants, two independent experiments, 2-min interval over 3–4 h), we also observed long leading processes with very dynamic growth cones, suggesting that neurite extension was normal[7] (data not shown). However, the forward movement of the nucleus was also perturbed. In this case, the centrosome appeared to stay too close to the nucleus and did not jump into the rostral swelling (**Figs. 5c** and **6d**,**e** and **Supplementary Videos 5** and **6** online), although this later formed and moved in the normal forward direction. The leading and trailing processes were not more branched than in wild-type granule cells (**Fig. 7**).

In vivo evidence for nucleus-centrosome uncoupling

We next tried to determine whether the abnormal distance between the centrosome and the nucleus is transient and whether it occurs *in vivo*. Cerebellar sections from adult wild-type, *Plxna2*$^{-/-}$ and *Sema6a*$^{-/-}$ mice were labeled with antibodies to α6 and to centrin 2 to visualize granule cells and centrosomes, respectively, whereas the nucleus was labeled with Hoechst. Confocal imaging was used to quantify the proportion of granule cells that had a nucleus that was not immediately adjacent to a centrosome (see Methods). In wild-type mice, only 10.9% of molecular layer interneurons (Hoechst positive and α6 negative, $n = 167$) and 14.1% of the granule cells in the IGL (Hoechst positive and α6 positive, $n = 912$) did not have their nucleus located near a centrosome (**Fig. 8**). These proportions were comparable in *Sema6a*$^{-/-}$

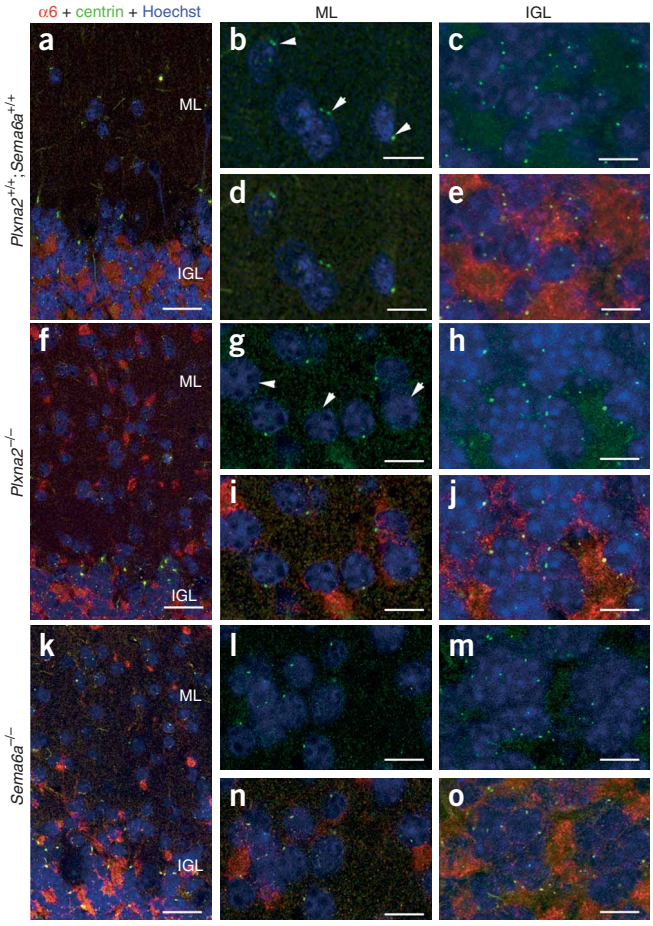

Figure 8 Nucleus-centrosome coupling *in vivo* in ectopic granule cells. Confocal images (2 μm) of adult cerebella immunostained with antibodies to α6 and centrin 2 and counterstained with Hoechst. (**a**–**e**) In wild type, all α6-expressing cells were in the IGL. The Hoechst-labeled nucleus of α6-negative molecular layer (ML) interneurons was always adjacent to a centrin 2–positive centrosome that appeared as one or two dots (arrowheads; **b**,**d**). Centrosome-nucleus distance in the IGL (**c**,**e**). Granule cells were all α6-positive. (**f**–**j**) Nucleus-centrosome distance in *Plxna2*$^{-/-}$ cerebellum. Many ectopic α6-positive granule cells were found in the molecular layer (**f**). Many nuclei of ectopic α6-positive granule cells (arrowheads) were not adjacent to a centrosome (**g**,**i**). Centrin 2/α6–labeling in the IGL of a *Plxna2*$^{-/-}$ mutant (**h**,**j**). (**k**–**o**) Nucleus-centrosome distance in *Sema6a*$^{-/-}$ cerebellum. Ectopic α6-positive granule cells were also found in the molecular layer, but most had a nucleus adjacent to a centrin 2–immunoreactive centrosome (**k**,**l**,**n**). Centrin 2/α6 labeling in the IGL of a *Sema6a*$^{-/-}$ mutant (**m**,**o**). Scale bars represent 20 μm (**a**,**f**,**k**) and 6 μm (**b**–**e**, **g**–**j**, **l**–**o**).

and *Plxna2*$^{-/-}$ mutants (**Fig. 8**) for molecular layer interneurons (11.7%, $n = 115$ and 4.9%, $n = 123$, respectively) and granule cells in the IGL (10.5%, $n = 935$ and 7%, $n = 1{,}087$, respectively). However, different results were obtained for ectopic granule cells. Although the proportion of ectopic granule cell nuclei not associated with a centrosome was comparable to IGL granule cells in *Sema6a*$^{-/-}$ mice (10.5% versus 11.7%, $n = 450$; **Fig. 8**), more than half of the molecular layer granule cells were not associated with a centrosome in *Plxna2*$^{-/-}$ mutants (53.2%, $n = 664$; **Fig. 8**). This suggests that nucleus-centrosome coupling is perturbed *in vivo* in the absence of plexin-A2.

DISCUSSION

Semaphorins and plexins were first noticed for their role in axon guidance, but were later shown to influence cell migration in normal and tumor cells[20,21]. How semaphorin-plexin signaling controls cell migration is still unclear. A recent study suggests that Sema3A attracts radially migrating cortical neurons and that type A plexins are involved[22]. We show here that the plexin-A2 receptor is expressed by postnatal granule cells and that, together with its ligand Sema6A, it controls their migration. In mice lacking one or both molecules, a defect of nucleus-centrosome coupling, as well as actin dynamics, blocks the initiation of radial migration (**Supplementary Fig. 5** online).

Plexin-A2/Sema6A controls centrosome-nucleus dynamics

It is still unclear as to how extracellular signals are detected and transduced from cell surface receptors to the migration machinery[23]. We provide direct genetic evidence suggesting that Sema6A–plexin-A2 signaling controls the transition from tangential to radial migration in cerebellar granule cells *in vivo*. In *Sema6A*$^{-/-}$ granule cells, the centrosome was unable to move forward and was closer to the nucleus than in wild-type granule cells, whereas the centrosome uncoupled from the nucleus in the absence of plexin-A2. This detachment of the centrosome may occur during tangential migration or at the beginning of radial migration. In both cases, however, the ectopic granule cells will be found in the molecular layer, as the EGL disappears in the adult cerebellum. The increased centrosome-nucleus spacing seemed to be permanent, as it was still observed in ectopic granule cells of adult *Plxna2*$^{-/-}$ cerebella. The different nucleus-centrosome coupling defects in *Sema6A*$^{-/-}$ and *plexin-A2*$^{-/-}$ granule cells are intriguing, although in both cases the end result is an inhibition of nuclear translocation. Because granule cells appeared to coexpress plexin-A2 and Sema6A at a stage of their migration in the EGL, one hypothesis for explaining these data would be that Sema6A inhibits plexin-A2 *in cis* and that plexin-A2 is overactive in the absence of Sema6A. In culture, this could cause an opposite effect on the centrosome. Sema6A might thus have two functions: one to act as a ligand to activate plexin-A2 and stimulate cell migration *in trans*, and a second to modulate plexin-A2 activity *in cis*. Removing Sema6A would block cell migration primarily by overactivating plexin-A2 *in cis*, leading to increased coupling of the centrosome and nucleus. Removing plexin-A2 would block cell migration by uncoupling the centrosome from the nucleus. An alternative explanation is that another plexin molecule is redundant with plexin-A2 as the receptor for Sema6A. In this case, the Sema6A–plexin-A2 pathway should be completely inactivated in *Sema6a*$^{-/-}$ cells, but still be partially active in *Plxna2*$^{-/-}$ cells. Thus, when the Sema6A–plexin-A2 pathway is completely inactivated, the migration of both the nucleus and the centrosome might be impaired; whereas when the Sema6A–plexin-A2 pathway is partially inactivated, the migration of the nucleus, but not the centrosome, might be affected.

A cell-autonomous receptor function for plexin-A2 is supported by the binding of the Sema6A ectodomain to plexin-A2–expressing cells[11] and the analysis of mouse chimeras and the *NMF454* ENU-mutant mice. In these mice, the alanine at position 396 in the extracellular domain of plexin-A2 is replaced by a glutamic acid. Notably, this alanine is evolutionarily conserved in plexin-A2 and plexin-A4, the two known receptors for Sema6A, and is absent from plexin-A1 and plexin-A3, which do not bind Sema6A (F.S. and H.F., unpublished data). On the basis of the existing data on the structure of the semaphorin domain[24], the mutation of alanine 396 should not affect the overall fold of the domain. This residue is probably part of the Sema6A-binding region, as Sema6A does not bind to a mutated

plexin-A2 protein bearing the A396E substitution. Our data support the importance of the semaphorin domain for plexin-A function *in vivo* and identify an amino acid required for direct semaphorin-plexin binding.

What links plexin-A2 and Sema6A to the centrosome and nucleus?

Our results suggest that neurite extension and polarity, as well as the perinuclear microtubule cage, were not primarily affected in Sema6A- or plexin-A2–deficient granule cells, whereas actin dynamics appeared to be perturbed in the absence of plexin-A2. Actin and its main partners, such as myosin II or cofilin, are known to control migration and, in particular, nuclear translocation[25–27]. Notably, application of cytochalasin on migrating granule cells or myosin II inhibition specifically block neuronal migration without affecting neurite extension, similar to what is seen in Sema6A or plexin-A2–deficient granule cells[26] (J.R. and A.C., unpublished data). In plexin-A2–deficient granule cells, defects in actin localization or polymerization may perturb myosin II function. It has been shown previously that actin contributes to Lis1-regulated soma translocation in granule cells[5,28], but microtubules also have a critical role in this process[29]. Therefore, it is likely that both actin and microtubule dynamics control Sema6A and plexin-A2 function in nuclear translocation.

It is still unclear how type A plexins regulate the actin cytoskeleton. Actin polymerization and the formation of contractile actin-myosin filaments are tightly controlled by Rho guanosine-5′-triphosphatases (RhoGTPases, including RhoA, Rac and Cdc42)[30]. Mounting evidence supports a role for RhoGTPases such as Rnd1 (refs. 31,32), Rac and RhoD[33,34] in signaling downstream of type A plexins. They also bind to modulators of RhoGTPases such as p190-RhoGAP[35] and the Rac-GEF FARP2 (ref. 36; FERM, RhoGEF and pleckstrin domain protein 2). It has been proposed that plexins carry out a regulatory role by sequestrating RhoGTPases and withdrawing these GTPases from the pool of active molecules that regulate the actin cytoskeleton[34]. For example, in the absence of plexin-A2 or stimulation of plexin-A2 by Sema6A, the level of available Rac could be increased, leading to hyperactivation of the Ser/Thr kinase PAK and subsequently modifying F-actin polymerization and actin-microtubule interactions. In addition, abnormal RhoGTPase activity, in particular that of Cdc42, may perturb partitioning-defective 6 (ref. 37), a protein that controls centrosome positioning and granule cell radial migration[3].

Signaling proteins other than RhoGTPases could also be involved. We showed here that Sema6A binding to plexin-A2 increases Cdk5 phosphorylation, as was previously found for Sema3A[15]. Many studies have linked Cdk5 to neuronal migration[38]. Notably, in *Cdk5*$^{+/+}$;*Cdk5*$^{-/-}$ mouse chimeras, ectopic *Cdk5*$^{-/-}$ granule cells are blocked in the molecular layer, as in *Sema6a*$^{-/-}$ and *Plxna2*$^{-/-}$ mice[39]. Moreover, Cdk5 regulates the microtubule cytoskeleton in migrating neurons (nucleus-centrosome coupling[40] and actin polymerization[41]). This involves Cdk5 substrates such as doublecortin, NudEL and p27^{kip1}. Therefore, abnormal Cdk5 activity or localization may contribute to the granule cell migration defects in *Sema6a*$^{-/-}$ and *Plxna2*$^{-/-}$ mice.

Neuronal migration proteins and psychiatric diseases

Mounting evidence suggests that many neurological diseases and psychiatric disorders, such as lissencephaly, schizophrenia and epilepsy, are associated with neuronal migration defects. Many of these have been linked to mutations in genes that encode proteins that are enriched at the centrosome or in the perinuclear microtubules[29,42–44]. Our data, together with other recent studies, suggest that plexin-A2 may be also involved in neuropsychiatric diseases. Indeed, genetic linkage and association studies in European, American[45] and Japanese[46] individuals with schizophrenia have identified *PLXNA2* as a candidate gene, although this had not been detected in a smaller Japanese cohort[47]. Likewise, an association between *PLXNA2* single-nucleotide polymorphism and anxiety has been described[48]. Abnormal cerebellum structure and function also seem to be associated with several neuropsychiatric disorders[49]. The phenotypes that we observed and the links to pathways that have been previously implicated in psychiatric or neurological disorders suggest that variants of Sema6A and plexin-A2 may also contribute to the risk of such disorders in humans.

METHODS

Animals. Swiss and C57BL6/J mice (Janvier) were used for expression studies. The *Plxna2*$^{-/-}$ line has been described elsewhere[11]. Mice were anesthetized with isofluorane (Abbott). The day of birth corresponds to postnatal day 0 (P0). All animal procedures were carried out in accordance with Université Pierre et Marie Curie guidelines.

ENU mice and *Plxna2* mutagenesis. *NMF454* mice were first identified in the G3 offspring in a previously described ENU-mutagenesis screen of C57BL6/J mice (http://nmf.jax.org/) by their smaller size and subtle ataxic gait. Because gait abnormalities were not apparent in all mutant mice, mouse phenotype was routinely determined by histology. To identify the mutation site (GATC Biotech AG), genomic DNA was extracted and all exons of the *Plxna2* gene were amplified by PCR using the GoTaqGreen MasterMix (Promega) in a GeneAmp PCR System 9700 cycler (Applied Biosystem). After sequencing, products were analyzed using ABI 3730XL DNA Analyzer (Applied Biosystem). The results were analyzed using SeqMan (DNASTAR-Lasergene, version 7.1). To determine whether Sema6A binding to plexin-A2 was affected by the A396E point mutation, we introduced a similar mutation (GCG to GAG) into the *Plxna2* cDNA using QuikChange II XL Site-Directed Mutagenesis Kit (Stratagene). As a forward primer, we used 5′-GCA GTG CAC CAA GGA GCC TGT CCC AAT CG-3′, and as a reverse primer, we used 5′-CGA TTG GGA CAG GCT CCT TGG TGC ACT GC-3′. The mutated construct (plexin-A2A396E) was fully sequenced, confirming that only the cytosine at position 1,187 was replaced by adenine.

Immunocytochemistry. Brains were collected as previously described[50]. We incubated 4% (wt/vol) paraformaldehyde–fixed brain sections with antibodies to mSema6A (1:200, R&D Systems), $GABA_A$ receptor α6 subunit (1:1,000, Chemicon), CaMKIV (1:500), NeuN (1:500, Chemicon), CaBP (1:1,000, SWANT), GFP (1:300, Molecular Probes) or plexin-A2 (ref. 11), followed by species-specific secondary antibodies (Jackson Immunoresearch). For centrosome staining, fresh frozen brains were cut with a cryostat (Leica) and 10-μm sections were fixed in methanol. Sections were immunostained with antibodies to α6 and centrin 2 (1:500, gift from M. Bornens, Curie Institute). Sections were counterstained with Hoechst 33258 (10 μg ml^{-1}; Sigma), mounted in Mowiol (Calbiochem) and examined with a fluorescent microscope (DMR, Leica) coupled to a CoolSnapFx camera (Roper Scientific) or a fluorescent confocal microscope (SP5, Leica).

BrdU injections and staining. P7 mice were injected intraperitoneally with BrdU (Sigma, 15 mg ml^{-1}, 50 mg per kg of body weight) diluted in a saline solution. Animals were perfused 36 h or 100 h after injection. Brain sections were incubated in 4 N HCl for 5 min at room temperature 21–25 °C and then with a mouse antibody to BrdU (1:100, Becton Dickinson), biotinylated antibody to mouse IgG (1:200, Amersham) and Vectastain ABC Kit (Vector Laboratories).

Binding assay. P10 fresh-frozen brain sections were fixed in cooled methanol for 30 min. After a blocking step in phosphate-buffered saline (PBS), 4 mM $MgCl_2$, 10% (vol/vol) foetal bovine serum (Invitrogen), sections were incubated with supernatant from plexin-A2–AP–transfected COS7 cells for 2 h and then fixed in 60% (wt/vol) acetone, 4% (wt/vol) paraformaldehyde and 20 mM HEPES for 2 min. Endogenous phosphatase were inactivated at 65 °C for 2 h in PBS. Ligand bound to sections was revealed in Tris pH 9.5, 5 mM $MgCl_2$, 100 mM NaCl, 0.3 g liter^{-1} 4-nitro blue tetrazolium chloride, 0.25 g liter^{-1}

5-bromo-4-chloro-3-indolyl-phosphate (Roche). Sema6A-AP binding on COS7 cells expressing plexin-A2 and plexin-A2A396E was carried out as previously described[11].

***In situ* hybridization.** *Plxna2* sense and antisense riboprobes were labeled as described previously[50] by *in vitro* transcription of cDNAs encoding mouse *Plxna2* and *Plxna4* (ref. 11). *In situ* hybridization was carried out as previously described[50].

Generation of chimeric animals. To generate *Plxna2*$^{-/-}$:*Plxna2*$^{+/+}$ chimeric mice, we first crossed *Plxna2*$^{-/-}$ mice with an EGFP transgenic mouse line[14]. To obtain chimeras, cells of the *GFP;Plxna2*$^{-/-}$ morulae were microinjected into *Plxna2*$^{+/+}$ or *Plxna2*$^{-/-}$ 8-cell-stage embryos. The embryos were cultured in M16 medium overnight to blastocysts and then transplanted into recipient mice. We also injected cells of the *Plxna2*$^{+/+}$;*GFP* morulae into *Plxna2*$^{-/-}$ embryos to obtain *Plxna2*$^{-/-}$: *Plxna2*$^{+/+}$;*GFP* chimeric mice.

Plxna2/Sema6a signaling. HEK293T cells (American Type Culture Collection) were transfected with expression vectors encoding plexin-A2 (ref. 11), Cdk5 (a gift of T. Oshima, Riken) and p35 (a gift from P. Mehlen, Centre National de la Recherche Scientifique) with Lipofectamine 2000 according to manufacturer's instructions (Invitrogen). After 24–48 h, cells were treated with 10, 100 or 300 ng ml^{-1} of recombinant human Sema6A-Fc (R&D Systems) for 10 min or with PBS as a control. After 24–48 h, 35 µg of cleared cell lysates in NP-40 lysis buffer (50 mM Tris HCl, pH 7.5, 150 mM NaCl, 1 mM EDTA, 0.5% NP-40), supplemented with protease inhibitor cocktail and phosphatase inhibitor cocktail 1 and 2 (Sigma), were separated by SDS-PAGE and analyzed by western blot. Protein concentration was measured using Bradford assays. For the preparation of cerebellum and neocortex lysates, the lysis buffer contained 1% (vol/vol) Triton X-100, 50 mM Tris HCl, pH 7.5, 150 mM NaCl, 1 mM EDTA, supplemented with protease and phosphatase inhibitors (Sigma). We used polyclonal antibodies (all were from Santa Cruz Biotechnology and all were used at a 1:200 dilution) to Cdk5 C-8, phospho Cdk5 (Tyr15), plexin-A2 H70 and plexin-A2 C18.

EGL microexplants culture. EGL microexplants cultures of P4 or P5 mice were prepared as described previously[7]. Cultures were stained with rhodamine-conjugated phalloidin, Hoechst 33342 (10 µg ml^{-1}, Sigma), antibodies to βIII-tubulin (Tuj-1, 1:1,000, Eurogentec), Sema6A (1:500), plexin-A2 (ref. 11), centrin-2 (1:500), GM-130 (1:600, BD Biosciences) or γ-tubulin (1:500, Sigma).

Cerebella electroporation. Cerebella were dissected from P5 mice. Centrin 1–GFP (a gift from M. Bornens) and pCX-EGFP (provided by M. Okabe, Osaka University) endofree plasmids were diluted in PBS containing 0.2% (wt/vol) Fastgreen at a concentration of 5 µg µl^{-1} and 2 µg µl^{-1}, respectively. DNA was injected into the cerebellum using glass pipettes (3–4 µl) at three different sites. Cerebellum was subjected to five electric pulses of 75 V with a duration of 50 ms and a delay between pulses of 450 ms using 10-mm electrodes (CUY650-10, Nepagene) connected to a CUY-21 electroporator (Nepagene). Explants were obtained as described above.

Time-lapse confocal microscopy. EGL microexplants were cultured in 35-mm dishes (Ibidi, Biovalley). Before imaging, 20 mM HEPES was added to the culture medium. Individual cells were imaged with a high-speed confocal microscope (resonant scanner SP5, 8,000 Hz) enclosed in a thermostated chamber (37 °C, Life Imaging Service). *z* stacks ($\Delta z = 1$ µm, ten sections) were obtained every 2 min using a 40× (1.25 NA) objective. Tracking was carried out using ImageJ (Manual tracking plugin).

Statistical analysis. To quantify distances between the nucleus and centrosome on tissue sections, images were acquired with a SP5 confocal microscope (Leica) driven by Leica Software 2.61. In centrin 2–labeled cells, the centrosome appears as one or two bright dots. *Z* acquisition of 2 µm was performed, and for each cell the presence or absence of the centrosome was checked on the two adjacent confocal planes, thus approximating the average thickness of a granule cell. For statistical analysis, we used a paired *t*-test (GraphPad Software) to compare two conditions. The paired *t*-test determined whether the *n* measured values differ from each other significantly. The levels of significance are indicated as follows: $^{***}P < 0.0001$, $^{**}P < 0.005$, $^{*}P < 0.01$. Compiled data are expressed as mean ± s.e.m.

Granule cell migration and neurite outgrowth analysis. Analysis was carried out with Metamorph (Molecular Devices). To measure migration rate, we delimited concentric areas of 50-, 100- or 200-µm width at increasing distances from the explant border. The number of Hoechst-labeled pixels in each area was counted and then expressed as a percentage of the total number of pixels. To evaluate the overall rate of migration, we counted the total number of Hoechst-labeled pixels surrounding the explant.

Maximal neurite length was estimated by measuring the three longest βIII-tubulin–positive neurites of each explant. Neuritic length was estimated by laying out a circle containing approximately 90% of the βIII-tubulin–positive neurites[7]. We also counted the total number of βIII-tubulin–positive neurites in the 750-µm perimeter explant border.

Note: Supplementary information is available on the Nature Neuroscience website.

ACKNOWLEDGMENTS

We thank H. Sakagami and H. Kondo for antibody to the β isoform of CaMKIV, M. Okabe for GFP transgenic mice, M. Bornens for centrin-GFP plasmid and antibodies to centrin, and L. Beverly-Staggs and L. Marquis for technical assistance with the *NMF454* mice, the production of which was supported by the US National Institutes of Health (NS041215 and NS35900). We also thank Y.E. Jones and R. Robinson for their help with the analysis of plexin-A2 structure and R. Schwartzmann for help with confocal microscopy studies. A.C. and G.K. were supported by the Association pour la Recherche sur le Cancer, the Fondation pour la Recherche Médicale (programme équipe FRM) and the Agence Nationale pour la Recherche (ANR Neurosciences). H.F. was supported by the 21st Century Centers of Excellence Program and Grants-in-Aid for Scientific Research Japan. K.J.M. was supported by a Science Foundation Ireland grant (01/F.1/B006). S.L.A. is an investigator of the Howard Hughes Medical Institute. This work was also supported by grants from CREST (F.S.) of the Japanese Science and Technology Agency. J.R. is recipient of a fellowship from the Région Ile-de-France.

AUTHOR CONTRIBUTIONS

J.R., G.K. and I.S. carried out the *in vivo* phenotypic analyses of knockout mice and the expression studies. J.R. performed the *in vitro* experiments. Y.Z. carried out the biochemical studies. C.F. generated the plexin-A2A396E construct and did the binding experiments. V.G. and J.R. performed the time-lapse microscopy and analyzed the confocal images. F.S. and H.F. obtained the *Plxna2* knockout and antibodies. K.J.M. provided the *Sema6a* knockout and helped in the writing of the manuscript. D.K. and S.L.A. generated the *NMF454* ENU-mutant and mapped the mutation to the *Plxna2* locus. K.S. and M.S. generated the mouse chimeras. A.C. and H.F. designed the study, prepared the figures and wrote the core of the manuscript.

Published online at http://www.nature.com/natureneuroscience
Reprints and permissions information is available online at http://npg.nature.com/reprintsandpermissions

1. Komuro, H. & Yacubova, E. Recent advances in cerebellar granule cell migration. *Cell. Mol. Life Sci.* **60**, 1084–1098 (2003).
2. Zmuda, J.F. & Rivas, R.J. Actin filament disruption blocks cerebellar granule neurons at the unipolar stage of differentiation *in vitro*. *J. Neurobiol.* **43**, 313–328 (2000).
3. Solecki, D.J., Model, L., Gaetz, J., Kapoor, T.M. & Hatten, M.E. Par6α signaling controls glial-guided neuronal migration. *Nat. Neurosci.* **7**, 1195–1203 (2004).
4. Umeshima, H., Hirano, T. & Kengaku, M. Microtubule-based nuclear movement occurs independently of centrosome positioning in migrating neurons. *Proc. Natl. Acad. Sci. USA* **104**, 16182–16187 (2007).
5. Kholmanskikh, S.S., Dobrin, J.S., Wynshaw-Boris, A., Letourneau, P.C. & Ross, M.E. Disregulated RhoGTPases and actin cytoskeleton contribute to the migration defect in Lis1-deficient neurons. *J. Neurosci.* **23**, 8673–8681 (2003).
6. Guan, C.B., Xu, H.T., Jin, M., Yuan, X.B. & Poo, M.M. Long-range Ca^{2+} signaling from growth cone to soma mediates reversal of neuronal migration induced by slit-2. *Cell* **129**, 385–395 (2007).
7. Kerjan, G. *et al.* The transmembrane semaphorin Sema6A controls cerebellar granule cell migration. *Nat. Neurosci.* **8**, 1516–1524 (2005).
8. Tamagnone, L. *et al.* Plexins are a large family of receptors for transmembrane, secreted and GPI-anchored semaphorins in vertebrates. *Cell* **99**, 71–80 (1999).
9. Toyofuku, T. *et al.* Guidance of myocardial patterning in cardiac development by Sema6D reverse signaling. *Nat. Cell Biol.* **6**, 1204–1211 (2004).

10. Suto, F. *et al.* Plexin-a4 mediates axon-repulsive activities of both secreted and transmembrane semaphorins and plays roles in nerve fiber guidance. *J. Neurosci.* **25**, 3628–3637 (2005).
11. Suto, F. *et al.* Interactions between plexin-A2, plexin-A4, and semaphorin 6A control lamina-restricted projection of hippocampal mossy fibers. *Neuron* **53**, 535–547 (2007).
12. Weyer, A. & Schilling, K. Developmental and cell type–specific expression of the neuronal marker NeuN in the murine cerebellum. *J. Neurosci. Res.* **73**, 400–409 (2003).
13. Sakagami, H., Umemiya, M., Kobayashi, T., Saito, S. & Kondo, H. Immunological evidence that the beta isoform of Ca^{2+}/calmodulin-dependent protein kinase IV is a cerebellar granule cell–specific product of the CaM kinase IV gene. *Eur. J. Neurosci.* **11**, 2531–2536 (1999).
14. Okabe, M., Ikawa, M., Kominami, K., Nakanishi, T. & Nishimune, Y. 'Green mice' as a source of ubiquitous green cells. *FEBS Lett.* **407**, 313–319 (1997).
15. Sasaki, Y. *et al.* Fyn and Cdk5 mediate semaphorin-3A signaling, which is involved in regulation of dendrite orientation in cerebral cortex. *Neuron* **35**, 907–920 (2002).
16. Bellion, A., Baudoin, J.P., Alvarez, C., Bornens, M. & Metin, C. Nucleokinesis in tangentially migrating neurons comprises two alternating phases: forward migration of the Golgi/centrosome associated with centrosome splitting and myosin contraction at the rear. *J. Neurosci.* **25**, 5691–5699 (2005).
17. Schaar, B.T. & McConnell, S.K. Cytoskeletal coordination during neuronal migration. *Proc. Natl. Acad. Sci. USA* **102**, 13652–13657 (2005).
18. Tsai, J.W., Bremner, K.H. & Vallee, R.B. Dual subcellular roles for LIS1 and dynein in radial neuronal migration in live brain tissue. *Nat. Neurosci.* **10**, 970–979 (2007).
19. Higginbotham, H., Tanaka, T., Brinkman, B.C. & Gleeson, J.G. GSK3beta and PKCzeta function in centrosome localization and process stabilization during Slit-mediated neuronal repolarization. *Mol. Cell. Neurosci.* **32**, 118–132 (2006).
20. Chedotal, A., Kerjan, G. & Moreau-Fauvarque, C. The brain within the tumor: new roles for axon guidance molecules in cancers. *Cell Death Differ.* **12**, 1044–1056 (2005).
21. Ding, S., Luo, J.H. & Yuan, X.B. Semaphorin-3F attracts the growth cone of cerebellar granule cells through cGMP signaling pathway. *Biochem. Biophys. Res. Commun.* **356**, 857–863 (2007).
22. Chen, G. *et al.* Semaphorin-3A guides radial migration of cortical neurons during development. *Nat. Neurosci.* **11**, 36–44 (2007).
23. Tsai, L.H. & Gleeson, J.G. Nucleokinesis in neuronal migration. *Neuron* **46**, 383–388 (2005).
24. Love, C.A. *et al.* The ligand-binding face of the semaphorins revealed by the high-resolution crystal structure of SEMA4D. *Nat. Struct. Biol.* **10**, 843–848 (2003).
25. Bellenchi, G.C. *et al.* N-cofilin is associated with neuronal migration disorders and cell cycle control in the cerebral cortex. *Genes Dev.* **21**, 2347–2357 (2007).
26. Rivas, R.J. & Hatten, M.E. Motility and cytoskeletal organization of migrating cerebellar granule neurons. *J. Neurosci.* **15**, 981–989 (1995).
27. Gomes, E.R., Jani, S. & Gundersen, G.G. Nuclear movement regulated by Cdc42, MRCK, myosin and actin flow establishes MTOC polarization in migrating cells. *Cell* **121**, 451–463 (2005).
28. Kholmanskikh, S.S. *et al.* Calcium-dependent interaction of Lis1 with IQGAP1 and Cdc42 promotes neuronal motility. *Nat. Neurosci.* **9**, 50–57 (2006).
29. Tanaka, T. *et al.* Lis1 and doublecortin function with dynein to mediate coupling of the nucleus to the centrosome in neuronal migration. *J. Cell Biol.* **165**, 709–721 (2004).
30. Jaffe, A.B. & Hall, A. Rho GTPases: biochemistry and biology. *Annu. Rev. Cell Dev. Biol.* **21**, 247–269 (2005).
31. Rohm, B., Rahim, B., Kleiber, B., Hovatta, I. & Puschel, A.W. The semaphorin 3A receptor may directly regulate the activity of small GTPases. *FEBS Lett.* **486**, 68–72 (2000).
32. Oinuma, I., Ishikawa, Y., Katoh, H. & Negishi, M. The Semaphorin 4D receptor plexin-B1 is a GTPase-activating protein for R-Ras. *Science* **305**, 862–865 (2004).
33. Turner, L.J., Nicholls, S. & Hall, A. The activity of the plexin-A1 receptor is regulated by Rac. *J. Biol. Chem.* **279**, 33199–33205 (2004).
34. Tong, Y. *et al.* Binding of Rac1, Rnd1 and RhoD to a novel Rho GTPase interaction motif destabilizes dimerization of the plexin-B1 effector domain. *J. Biol. Chem.* **282**, 37215–37224 (2007).
35. Barberis, D. *et al.* p190 Rho-GTPase activating protein associates with plexins and it is required for semaphorin signaling. *J. Cell Sci.* **118**, 4689–4700 (2005).
36. Toyofuku, T. *et al.* FARP2 triggers signals for Sema3A-mediated axonal repulsion. *Nat. Neurosci.* **8**, 1712–1719 (2005).
37. Etienne-Manneville, S. & Hall, A. Integrin-mediated activation of Cdc42 controls cell polarity in migrating astrocytes through PKCzeta. *Cell* **106**, 489–498 (2001).
38. Xie, Z., Samuels, B.A. & Tsai, L.H. Cyclin-dependent kinase 5 permits efficient cytoskeletal remodeling—a hypothesis on neuronal migration. *Cereb. Cortex* **16** Suppl 1, i64–i68 (2006).
39. Ohshima, T. *et al.* Migration defects of *cdk5*$^{-/-}$ neurons in the developing cerebellum is cell autonomous. *J. Neurosci.* **19**, 6017–6026 (1999).
40. Xie, Z., Sanada, K., Samuels, B.A., Shih, H. & Tsai, L.H. Serine 732 phosphorylation of FAK by Cdk5 is important for microtubule organization, nuclear movement and neuronal migration. *Cell* **114**, 469–482 (2003).
41. Kawauchi, T., Chihama, K., Nabeshima, Y. & Hoshino, M. Cdk5 phosphorylates and stabilizes p27kip1 contributing to actin organization and cortical neuronal migration. *Nat. Cell Biol.* **8**, 17–26 (2006).
42. Clapcote, S.J. *et al.* Behavioral phenotypes of Disc1 missense mutations in mice. *Neuron* **54**, 387–402 (2007).
43. Shu, T. *et al.* Ndel1 operates in a common pathway with LIS1 and cytoplasmic dynein to regulate cortical neuronal positioning. *Neuron* **44**, 263–277 (2004).
44. Sasaki, S. *et al.* Complete loss of Ndel1 results in neuronal migration defects and early embryonic lethality. *Mol. Cell. Biol.* **25**, 7812–7827 (2005).
45. Mah, S. *et al.* Identification of the semaphorin receptor PLXNA2 as a candidate for susceptibility to schizophrenia. *Mol. Psychiatry* **11**, 471–478 (2006).
46. Takeshita, M. *et al.* Genetic examination of the *PLXNA2* gene in Japanese and Chinese schizophrenics. *Schizophr. Res.* **99**, 359–364 (2008).
47. Fujii, T. *et al.* Failure to confirm an association between the PLXNA2 gene and schizophrenia in a Japanese population. *Prog. Neuropsychopharmacol. Biol. Psychiatry* **31**, 873–877 (2007).
48. Wray, N.R. *et al.* Anxiety and comorbid measures associated with PLXNA2. *Arch. Gen. Psychiatry* **64**, 318–326 (2007).
49. Fatemi, S.H., Reutiman, T.J., Folsom, T.D. & Sidwell, R.W. The role of cerebellar genes in pathology of autism and schizophrenia. *Cerebellum* published online doi:10.1080/14734220701392969 (16 May 2007).
50. Marillat, V. *et al.* Spatiotemporal expression patterns of *slit* and *robo* genes in the rat brain. *J. Comp. Neurol.* **442**, 130–155 (2002).